

Supporting Information

Synthesis and Magnetic Studies of Pentagonal Bipyramidal Metal Complexes of Fe, Co and Ni

Yi-Fei Deng,^a Binling Yao,^a Peng-Zhi Zhan,^a Dexuan Gan,^a Yuan-Zhu Zhang^{*a} and Kim R. Dunbar^{*b}

^aDepartment of Chemistry, Southern University of Science and Technology, Shenzhen, 518000, China.

^bDepartment of Chemistry, Texas A & M University, College Station, TX 77842, USA.

Table S1. Selected bond lengths (Å) and angles (deg) for complexes **1-3**.

1		2		3	
Fe(1)-N(1)	2.121(3)	Co(1)-N(1)	2.123(2)	Ni(1)-N(1)	1.982(4)
Fe(1)-N(2)	2.176(3)	Co(1)-N(2)	2.171(2)	Ni(1)-N(2)	2.109(3)
Fe(1)-N(3) _{MeCN}	2.165(3)	Co(1)-N(3) _{MeCN}	2.120(2)	Ni(1)-N(3) _{MeCN}	2.048(3)
Fe(1)-O(1)	2.300(2)	Co(1)-O(1)	2.273(2)	Ni(1)-O(1)	2.477(3)
N(1)-Fe(1)-N(2)	73.03(7)	N(3)-Co(1)-N(3)#1	173.21(8)	N(1)-Ni(1)-N(3)#1	95.37(7)
N(1)-Fe(1)-N(3)	93.88(7)	N(3)-Co(1)-N(1)	93.40(4)	N(1)-Ni(1)-N(3)	95.37(7)
N(3)-Fe(1)-N(2)	90.93(10)	N(3)#1-Co(1)-N(1)	93.40(4)	N(3)#1-Ni(1)-N(3)	169.26(15)
N(1)-Fe(1)-N(3)#1	93.87(7)	N(3)-Co(1)-N(2)	90.68(6)	N(1)-Ni(1)-N(2)	77.06(8)
N(3)#1-Fe(1)-N(3)	172.25(14)	N(3)#1-Co(1)-N(2)	91.34(6)	N(3)#1-Ni(1)-N(2)	91.77(11)
N(3)#1-Fe(1)-N(2)	91.34(10)	N(1)-Co(1)-N(2)	72.70(4)	N(3)-Ni(1)-N(2)	90.63(11)
N(1)-Fe(1)-N(2)#1	73.03(7)	N(1)-Co(1)-N(2)#1	72.70(4)	N(1)-Ni(1)-N(2)#1	77.06(8)
N(2)-Fe(1)-N(2)#1	146.05(15)	N(2)-Co(1)-N(2)#1	145.40(9)	N(2)-Ni(1)-N(2)#1	154.11(16)
N(1)-Fe(1)-O(1)	144.92(5)	N(3)-Co(1)-O(1)#1	89.88(6)	N(1)-Ni(1)-O(1)	147.81(5)
N(3)#1-Fe(1)-O(1)	89.80(9)	N(3)-Co(1)-O(1)	84.54(6)	N(3)#1-Ni(1)-O(1)	89.22(9)
N(3)-Fe(1)-O(1)	83.85(9)	N(1)-Co(1)-O(1)#1	145.07(3)	N(3)-Ni(1)-O(1)	81.67(9)
N(2)-Fe(1)-O(1)	72.02(9)	N(2)-Co(1)-O(1)#1	142.08(6)	N(2)-Ni(1)-O(1)	70.96(10)
N(2)#1-Fe(1)-O(1)	141.86(9)	N(3)#1-Co(1)-O(1)	89.89(6)	N(2)#1-Ni(1)-O(1)	134.86(9)
N(1)-Fe(1)-O(1)#1	144.92(5)	N(1)-Co(1)-O(1)	145.07(3)	N(3)-Ni(1)-O(1)#1	89.22(9)
N(3)-Fe(1)-O(1)#1	89.80(9)	N(2)-Co(1)-O(1)	72.46(6)	N(1)-Ni(1)-O(1)#1	147.82(7)
N(2)-Fe(1)-O(1)#1	141.86(9)	N(2)#1-Co(1)-O(1)	142.08(6)	N(2)-Ni(1)-O(1)#1	134.86(9)
O(1)-Fe(1)-O(1)#1	70.16(10)	O(1)#1-Co(1)-O(1)	69.86(7)	O(1)-Ni(1)-O(1)#1	64.37(8)

Symmetry transformations used to generate equivalent atoms: #1 -x+1, y, -z+1/2.

Table S2. Parameters fitted for **1** at 1500 Oe and **2** at 1200 Oe by a generalized Debye model.

1			2		
<i>T</i> / K	τ / s	α	<i>T</i> / K	τ / s	α
2.00	$1.71(6) \times 10^{-3}$	0.27(2)	2.00	$9.85(2) \times 10^{-2}$	0.27(2)
2.25	$1.42(3) \times 10^{-3}$	0.21(1)	2.50	$2.47(4) \times 10^{-2}$	0.15(2)
2.50	$1.18(2) \times 10^{-3}$	0.17(1)	3.00	$7.81(2) \times 10^{-3}$	0.087(5)
2.75	$9.50(7) \times 10^{-4}$	0.14(1)	3.50	$2.88(3) \times 10^{-2}$	0.063(5)
3.00	$7.46(6) \times 10^{-4}$	0.13(1)	4.00	$1.25(1) \times 10^{-2}$	0.049(3)
3.25	$5.72(4) \times 10^{-4}$	0.096(4)	4.25	$8.65(4) \times 10^{-4}$	0.044(2)
3.50	$4.02(2) \times 10^{-4}$	0.069(3)	4.50	$6.12(3) \times 10^{-4}$	0.043(3)
3.65	$3.05(2) \times 10^{-4}$	0.057(3)	4.75	$4.48(2) \times 10^{-4}$	0.033(3)
3.80	$2.22(1) \times 10^{-4}$	0.042(3)	5.00	$3.32(2) \times 10^{-4}$	0.029(2)
3.95	$1.49(2) \times 10^{-4}$	0.041(4)	5.25	$2.50(3) \times 10^{-4}$	0.024(3)
4.10	$9.41(2) \times 10^{-5}$	0.052(5)	5.50	$1.90(1) \times 10^{-4}$	0.023(2)
4.25	$5.95(3) \times 10^{-5}$	0.054(6)	5.75	$1.45(2) \times 10^{-4}$	0.019(2)
4.50	$2.89(3) \times 10^{-5}$	0.067(4)	6.00	$1.11(2) \times 10^{-4}$	0.016(3)
			6.25	$8.38(4) \times 10^{-5}$	0.019(3)

Table S3. The SH parameters extracted from fitting and *ab initio* calculations for complexes **1–3**.

	<i>D</i> / cm ⁻¹	<i>E/D</i>	<i>g_x</i>	<i>g_y</i>	<i>g_z</i>
1	-19.7	0.02	2.13	2.17	2.65
2	+37.8	<0.01	2.30	2.28	2.04
3	-15.4	0.21	1.74	1.91	2.59

Table S4. The relative energies of ground and low-lying quartet spin eigenstates (cm⁻¹).

	1	2	3
⁴ Ψ ₀	0.0	0.0	0.0
⁴ Ψ ₁	5239.1	3078.2	6240.6
⁴ Ψ ₂	7612.3	3122.0	7394.0
⁴ Ψ ₃	9012.4	5282.6	8466.9
⁴ Ψ ₄	10367.1	5813.2	12385.7
⁴ Ψ ₅	11478.3	10392.2	12710.1
⁴ Ψ ₆	11961.4	13131.0	13109.3
⁴ Ψ ₇	24127.6	17262.0	28002.8
⁴ Ψ ₈	25364.1	18418.1	28268.5
⁴ Ψ ₉	27498.3	19842.2	29112.9

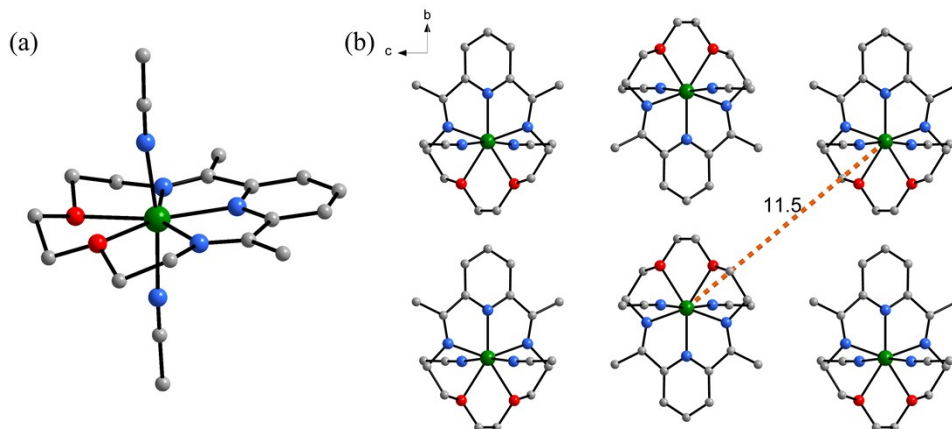


Figure S1. Molecular structure (a) and packing arrangement (b) of **1** along the crystallographic *a* axis; The dashed line shows the nearest intermolecular Fe...Fe separation (Å). Hydrogen atoms and counterions are omitted for clarity. Colour codes: Fe, green; C, grey; O, red; N, blue.

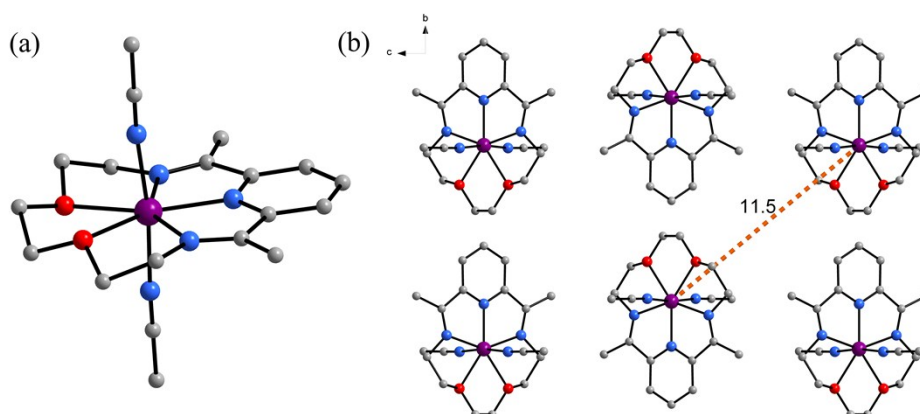


Figure S2. Molecular structure (a) and packing arrangement (b) of **2** along the crystallographic *a* axis; The dashed line shows the nearest intermolecular Co...Co separation (Å). Hydrogen atoms and counterions are omitted for clarity. Colour codes: Co, purple; C, grey; O, red; N, blue.

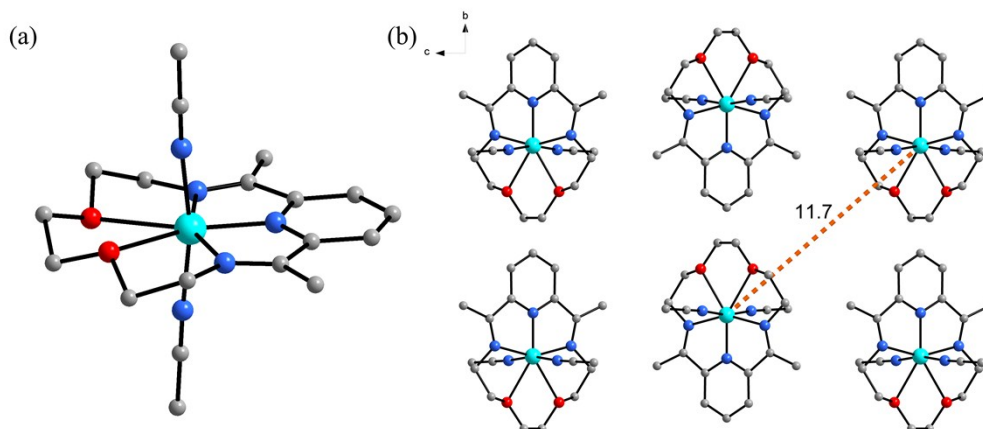


Figure S3. Molecular structure (a) and packing arrangement (b) of **3** along the crystallographic *a* axis; The dashed line shows the nearest intermolecular Ni...Ni separation (Å). Hydrogen atoms and counterions are omitted for clarity. Colour codes: Ni, green; C, grey; O, red; N, blue.

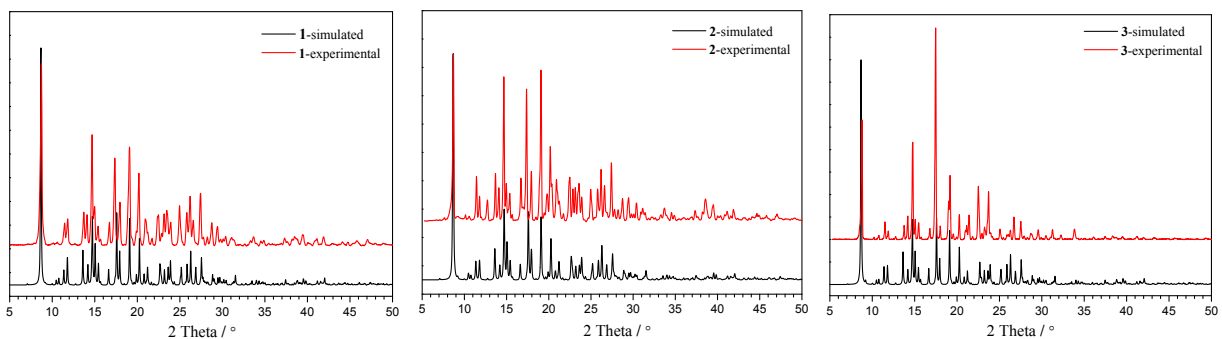


Figure S4. The powder X-ray diffractions for complexes 1-3. The black curve is calculated from the single crystal data.

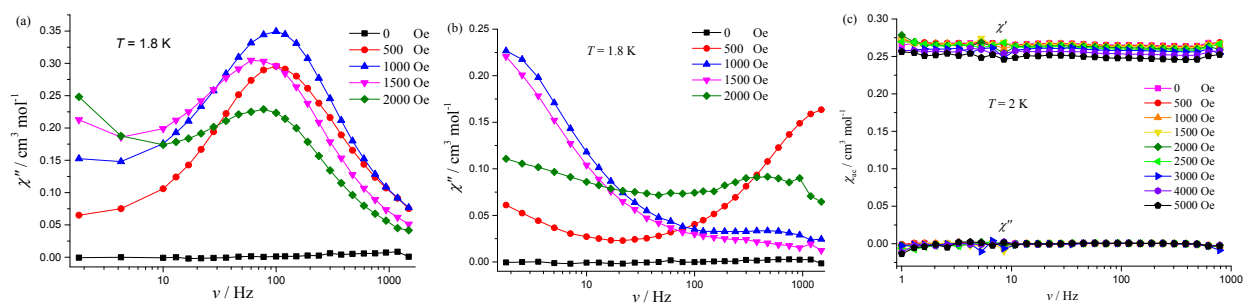


Figure S5. Frequency dependence of the ac susceptibility for 1(a), 2(b) and 3(c) under different dc fields. The lines are guides to the eyes.

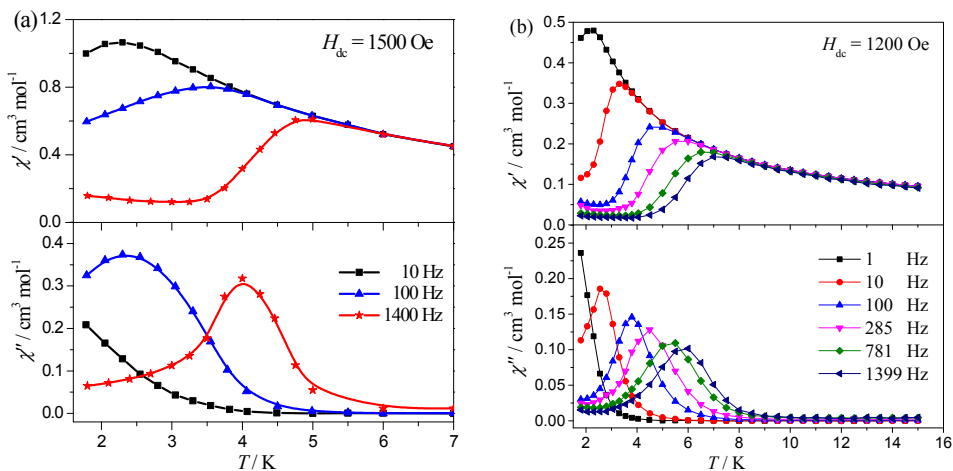


Figure S6. Temperature dependence of the in-phase (χ') and out-of-phase (χ'') ac susceptibility for 1(a) and 2(b) at indicated dc field. The lines are guides to the eyes.

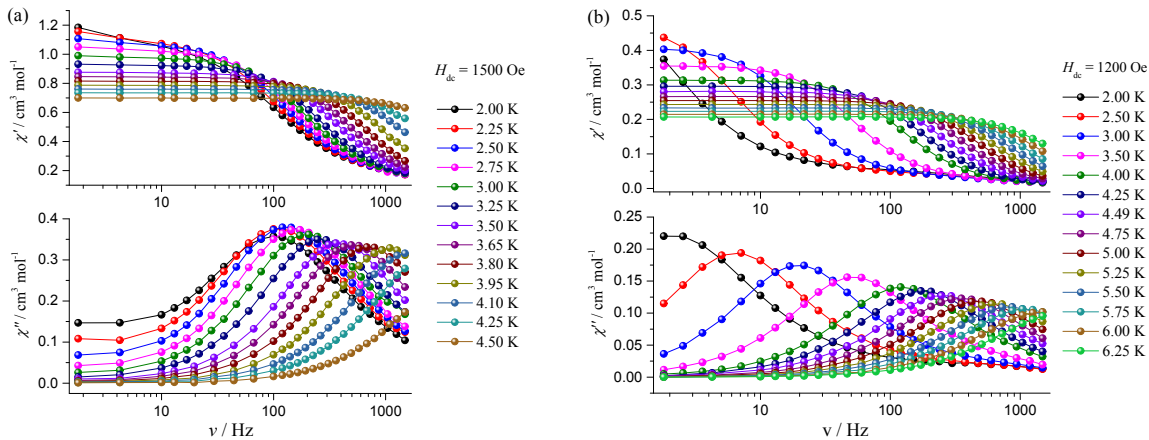


Figure S7. Frequency dependence of the in-phase χ' (top) and out-of-phase χ'' (bottom) components of the ac susceptibility for **1(a)** and **2(b)** at indicated dc field. The lines are guides to the eyes.

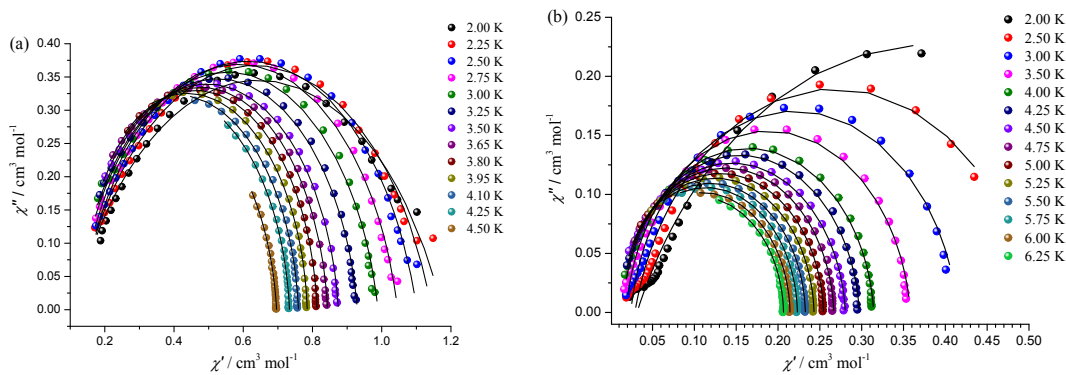


Figure S8. Cole-Cole plots for complexes **1(a)** and **2(b)**. The solid lines represent the fit to the data.

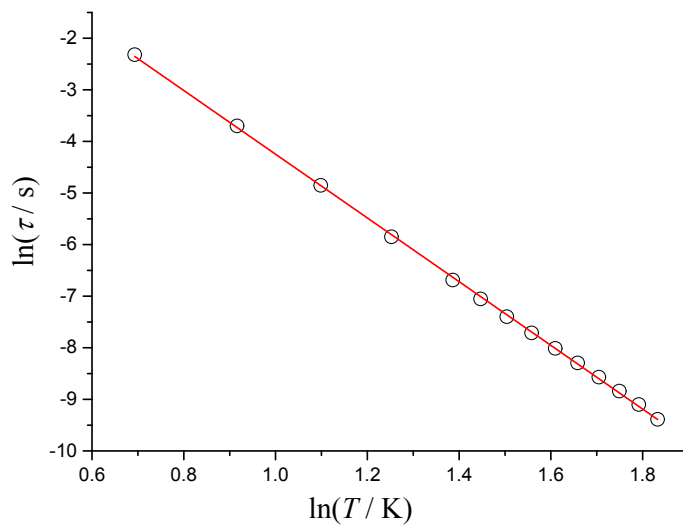


Figure S9. Power law analysis of complex **2** in the form $\ln(\tau)$ vs $\ln(T)$. The solid line represents the best fits to the data.